

Low-energy-electron-diffraction structural determination of the graphite (0001) surface

N. J. Wu* and A. Ignatiev

Department of Physics, University of Houston, Houston, Texas 77004

(Received 28 September 1981; revised manuscript received 23 November 1981)

Low-energy-electron-diffraction intensity-energy spectra obtained from the (0001) face of graphite have been compared to dynamical-scattering calculations for models of a reconstructed and unreconstructed surface. Agreement is found via r -factor analysis for the model assuming the bulk layer stacking sequence ($ABAB \dots$) at the surface and a top carbon layer contraction of 0.05 \AA (1.5% of the bulk value) and a surface nearly devoid of monatomic steps.

I. INTRODUCTION

Graphite is a highly anisotropic crystal in terms of its structural and electronic properties. With respect to its structural properties, it has been widely used as a substrate for studying phase transitions of physisorbed gases¹⁻³ and also as an ideal host lattice for studying the quasi-two-dimensional behavior in intercalation compounds.⁴⁻⁶ The two-dimensional (2D) structure of the clean graphite (0001) surface, however, has not been studied in detail. Past surface studies of graphite consist primarily of dated work concerned with the compilation of low-energy-electron-diffraction (LEED) I - V data for the (00) reflected beam^{7,8} and some work on pyrographite.⁹ The lack of meaningful LEED analyses at that time prevented complete structural determination for the graphite (0001) surface. However, over the past decade, significant advances have been made in surface crystallography by LEED allowing for the complete analysis of surface structures. In light of this, and of our current interest in adsorption of alkali metals on graphite,¹⁰ we have undertaken the LEED characterization of the atomic structure of the graphite (0001) surface.

II. EXPERIMENTAL

The experimental apparatus consists of a UHV chamber (pressure $\sim 1 \times 10^{-10}$ Torr) in which are mounted a standard four grid LEED optics (also used with an external electron gun as a retarding field electron-energy analyzer for Auger spectroscopy), a sputter ion gun, a quadrupole mass spectrometer, and a universal manipulator for sample heating and cooling and precise sample positioning in the UHV chamber. Natural graphite crystal platelets 2-4 mm in diameter were initially cleaved in air with a dry nitrogen gas stream. A sample was then mounted on the manipulator, placed in the vacuum chamber and a clean and a large grain defined by Auger electron spectroscopy (AES) and LEED prior to baking the

vacuum chamber. If a large clean grain could not be found, the sample was recleaved in air (as there was no provision for cleaving in vacuum) and the procedure repeated. If no impurity Auger peaks were discernable above the noise level after baking the chamber (to 200°C), the experiment was continued. It should be noted that the standard surface cleaning procedures of inert gas ion bombardment and high-temperature heating in vacuum damage the surface of the graphite to the extent of making it unusable for LEED structural determination. Therefore, cleaving is the appropriate procedure for obtaining a clean surface which, we have observed, is generally very stable to contamination even when cleaved in air.

After defining a large, clean grain on the graphite sample, the grain surface was aligned normal to the incident electron beam by the criterion that the intensity profiles of symmetric beams, i.e., the (10), (0 $\bar{1}$), and ($\bar{1}$ 1); or the (01), ($\bar{1}$ 0), and (1 $\bar{1}$) (see Fig. 1), were identical to each other to within a few percent.

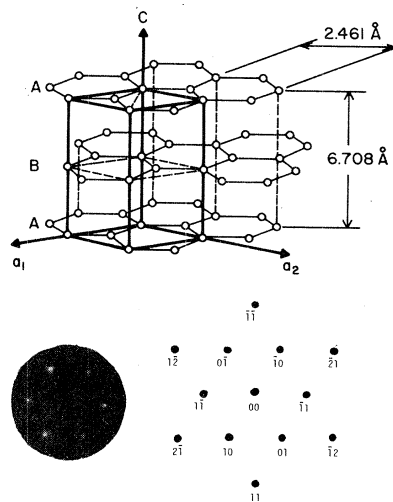


FIG. 1. The real-space structure, 2D reciprocal lattice, and LEED pattern at 120 eV. Note the threefold symmetry in the pattern.

First- and second-order diffracted beam intensities were measured with the sample at room temperature from the fluorescent screen via spot photometer and plotted directly on an x - y recorder. The experimental intensity profiles were then normalized to the incident beam current via computer.

III. LEED Analysis

A. Structural models

Pure graphite is characterized by a layered structure with an hcp lattice ($ABAB \dots$ stacking). The single layer has a honeycomb structure, i.e., a hexagonal arrangement without a center atom with the surface unit cell being a two-dimensional parallelogram with a lattice constant $a = 2.46 \text{ \AA}$ and two carbon atoms per unit cell (see Fig. 1). The hcp structure for graphite and the limited penetration depth of low-energy electrons will result in a threefold symmetric LEED pattern for the (0001) surface if only one surface termination (A or B) is present. All hcp (0001) surfaces studied to date, however, have shown sixfold symmetric patterns as a result of both A and B terminations being present on the surface as a result of the presence of atomic steps and the resulting averaging of the two threefold patterns.¹¹ Figure 1 shows the LEED pattern for the present nitrogen cleaved (0001) graphite sample to be threefold symmetric. This indicates that over the $\sim 1\text{-mm}^2$ area of the incident beam the graphite grain sampled had essentially a single termination, i.e., little or no atomic steps present at the surface. This will be later commented on in the analysis of the diffracted intensities, however, it is well to note here that the lack of monatomic steps on the graphite surface is very dependent on the cleaving procedure used. Cleaves using "Scotch" tape or a razor blade have produced samples with sixfold symmetry and therefore with enough monatomic steps on the surface to give approximately equal amounts of both A and B terminations of graphite.

In this work, we have evaluated two kinds of model geometries for the graphite (0001) surface. Bulk graphite-layer stacking is in the $ABAB \dots$ sequence. We have utilized this bulk stacking sequence for the first of the structural models for the graphite surface. It has been reported, however, that in stage-1 intercalates the stacking of the graphite layers goes to $AAA \dots$ with usually alkali-metal atom layers in between. In light of this stacking change because of a significant perturbation of the system (intercalant atoms), we have, in addition to the bulk stacked $ABAB \dots$ structure, considered a structure with stacking sequence $AABAB \dots$, where the reconstruction may occur as a result of the perturbation of the surface on the system. In addition, it has been previously reported that a number of layered compounds exhibit surface relaxation.¹²⁻¹⁴ As gra-

phite has a large interlayer spacing ($d_z = 3.35 \text{ \AA}$), we varied the first interlayer spacing in our models from -6% to $+6\%$ of d_z (-0.20 to $+0.20 \text{ \AA}$) to determine any surface relaxation present.

B. LEED calculations

Full dynamical LEED calculations similar to those recently used by VanHove and Somorjai in studying hydrogenless benzene molecules¹⁵ were performed for the above models. The multiple scattering within each layer, where there are two atoms per unit cell, was treated with the reverse scattering perturbation (RSP) method.¹⁶ While for the interlayer scattering, the renormalized forward scattering¹⁷ (RFS) was used. The phase shifts used for carbon were those generated by Kesmodel *et al.*¹⁸ for C_2H_2 and C_2H_4 , with five phase shifts being used. It should be noted that using the carbon phase shifts previously used¹⁹ for CO gave poor agreement between theory and experiment. A surface Debye temperature of 973 K was used. The imaginary part of the inner potential was set to -5 eV , and the real component of the inner potential was varied to obtain the best correspondence with the totality of the data. This variation produced a -8.2-eV value for the inner potential. Twenty-two symmetry reduced beams were used in the energy region of calculation. It is well to note that since the LEED pattern was threefold symmetric, no averaging of calculated terms was required for comparison of experiment.

C. Result and discussion

Figures 2 and 3 show a comparison between the experimentally determined I - V curves for graphite and the calculated ones with assumed $ABAB \dots$

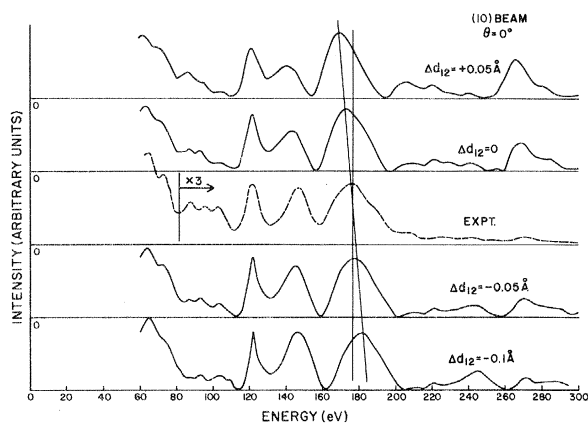


FIG. 2. Intensity-energy spectra for the (10) beam at normal incidence. Dashed curve—experiment; solid curve—calculations for varying top carbon-layer spacing, d_{12} . Note the systematic shift to lower energy of the peak at $\sim 180 \text{ eV}$ with increasing top-layer spacing.

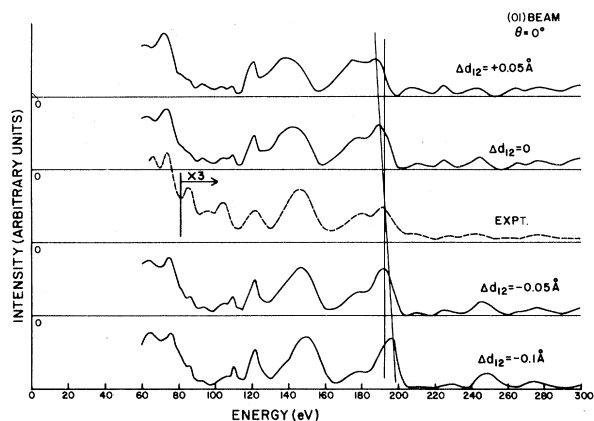


FIG. 3. Intensity-energy spectra of the (01) beam at normal incidence. Dashed curve—experiment; solid curve—calculations for varying top carbon-layer spacing, d_{12} . Note the differences between the (01) beam spectra and the (10) beam spectra of Fig. 2, giving the observed threefold symmetry of the diffraction pattern.

stacking and a single termination of the surface. At normal incidence, the first-order beams show threefold symmetry (compared Figs. 2 and 3) with the very good agreement between calculation and experiment giving further credibility to the single termination description of the cleaved graphite surface. The second-order beams at normal incidence show sixfold symmetry due to the diperiodicity of the graphite-layer stack. The intensity profiles of the (00) diffracted beams have also been measured at 5° , 6° , 7° , and 8° from normal incidence and have the same peak locations and intensity distributions as that observed previously.^{7,8}

As noted, the intensity calculations were carried out for various values of the distance between the first and second layers, d_{12} . The results for *ABAB* . . . stacked graphite are presented as solid curves in Figs. 2 and 3. Note that the calculated intensity distributions have quite large peak shifts with change in top-layer spacing (about 10 eV for 3% change) and some shape change with top-layer spacing change. The large and systematic peak shift with interlayer spacing change [cf. (10) beam at ~ 180 eV] indicates a high sensitivity of the calculations to surface relaxation and hence points to a straightforward and accurate method for determining surface relaxation in graphite. For the *ABAB* . . . stacking, this results in determination of a top-layer contraction of 0.05 \AA : a 1.5% bond-length contraction with respect to the bulk value. In graphite with its alternating stacking sequence (*ABAB* . . .), there is a strong *SP*² bonding of the carbon atoms in the plane and weak Van der Waals coupling between the planes. The slight contraction of the first Van der Waals spacing in graphite surface is similar to that observed for other Van der Waals bonded layer com-

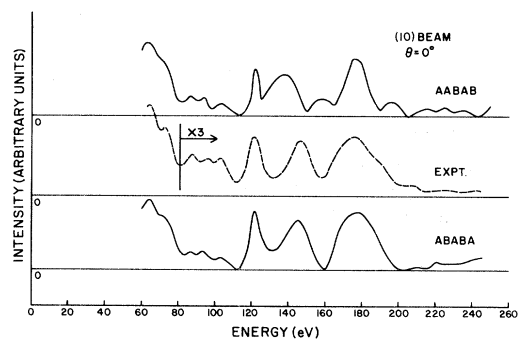


FIG. 4. Intensity-energy spectra for the (10) beam at normal incidence and $d_{12} = 3.30 \text{ \AA}$ as a function of surface structural model. Dashed curve—experiment; *ABABA* . . . solid curve—calculations assuming bulklike *ABABA* . . . stacking of carbon layers; *AABAB* . . . solid curve—calculations assuming surface reconstruction to an *AABAB* . . . stacking.

pounds.¹²⁻¹⁴

r-factor analysis was applied to the *ABAB* . . . stacking calculations and experiment for the three measured beams at normal incidence. The Zanazzi-Jona²⁰ *r* factor was used and yielded a total value of 0.19 for the 0.05 \AA contracted surface indicating very good agreement between theory and experiment.

Figure 4 gives the calculated results for the reconstructed surface model with the stacking sequence, *AABAB* . . . It shows a four-peak structure in the (10) beam in the 130–210-eV region as compared to the two-peak structure in the (10) beam calculated for the *ABAB* . . . stacking and observed in experiment. This, along with similar behavior in the (01) beam, gives poorer agreement with experiment than Figs. 2 and 3 as witnessed by the poorer 0.35 *r*-factor value for this model. It is expected that *AABAB* . . . stacking would force a larger top-layer spacing for the surface than the *ABAB* . . . stacking sequence.²¹ Examination of the calculations, however, reveals that the more the top-layer spacing d_{12} is expanded, the more striking the disagreement between calculation and experiment. It is evident, therefore, that this reconstruction of a shear displacement of adjacent carbon layers does not exist at the clean graphite surface.

IV. CONCLUSION

The atomic structure of the clean (0001) graphite surface has been determined by LEED. Bulk *ABAB* . . . stacking is found to exist at the surface with a 0.05-\AA contraction of the top carbon-layer spacing as determined by *r*-factor analysis (total *r* fac-

tor = 0.19). In addition, the threefold symmetric property of the diffraction pattern and the excellent agreement to calculations assuming only one termination for the surface indicate that the cleaved sample was nearly devoid of monoatomic steps. Such a property is extremely beneficial for the future interpretation of phase transitions of adsorbates¹⁰ on the (0001) graphite surface.

ACKNOWLEDGMENTS

We gratefully acknowledge helpful discussions with Dr. M. Passler and Dr. S. Moss who also supplied the graphite samples used in this study. Partial support for this work has been supplied by the R. A. Welch Foundation and the Petroleum Research Fund as administered by the American Chemical Society.

*Permanent address: Institute of Physics, Academia Sinica, Beijing, China.

- ¹H. Taub, C. Passell, J. K. Kjems, K. Carneiro, J. P. McTague, and J. G. Dash, *Phys. Rev. Lett.* **34**, 654 (1975).
²C. G. Shaw, S. C. Fain, and M. D. Chinn, *Phys. Rev. Lett.* **41**, 955 (1978).
³S. C. Fain, M. D. Chinn, and D. R. Diehl, *Phys. Rev. B* **21**, 4170 (1980).
⁴G. S. Parry, *Mater. Sci. Eng.* **31**, 99 (1977).
⁵N. Kambe, G. Dresselhaus, and M. Dresselhaus, *Phys. Rev. B* **21**, 3991 (1980).
⁶S. C. Moss and H. Zabel, *Surf. Sci.* **97**, L357 (1980).
⁷J. J. Lander and J. Morrison, *J. Appl. Phys.* **35**, 3593 (1964).
⁸E. G. McRae and C. W. Caldwell, Jr., *Surf. Sci.* **7**, 41 (1967).
⁹S. Goldsztaub, in *Proceedings of the 7th International Conference on Electron Microscopy, Grenoble, France, 1970* (unpublished); *Acta Crystallogr. Sect. A* **28**, S205 (1972).

- ¹⁰N. J. Wu and A. Ignatiev (unpublished).
¹¹F. Jona, *J. Phys. C* **11**, 4271 (1978).
¹²B. Mrstik, R. Kaplan, T. Reineche, M. A. VanHove, and S. Y. Tong, *Phys. Rev. B* **15**, 897 (1977).
¹³B. Lau, B. Mrstik, S. Y. Tong, and M. A. VanHove (unpublished).
¹⁴M. A. VanHove, S. Y. Tong, and M. Elconin, *Surf. Sci.* **69**, 85 (1977).
¹⁵M. A. VanHove and G. Somorjai (unpublished).
¹⁶J. B. Pendry, *Low Energy Electron Diffraction* (Academic, London, 1974).
¹⁷M. A. VanHove and S. Y. Tong, *Surface Crystallography by LEED* (Springer, Heidelberg, 1979).
¹⁸L. L. Kesmodel, K. C. Baetzeld, and G. A. Somorjai, *Surf. Sci.* **66**, 299 (1977).
¹⁹M. Passler, A. Ignatiev, F. Jona, D. Jepsen, and P. M. Marcus, *Phys. Rev. Lett.* **43**, 360 (1979).
²⁰E. Zanazzi and F. Jona, *Surf. Sci.* **62**, 61 (1976).
²¹J. Fisher and T. Thompson, *Phys. Today* **31(7)**, 36 (1978).

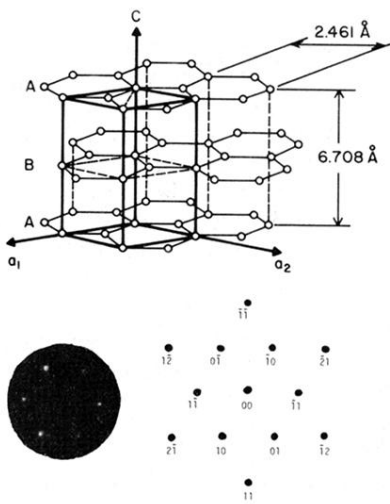


FIG. 1. The real-space structure, 2D reciprocal lattice, and LEED pattern at 120 eV. Note the threefold symmetry in the pattern.